

On Energy Optimal Speed Trajectories in Urban Traffic: Implementation Options

1st Eduardo Fernando Mello
 Department of Electrical Engineering
 University of Notre Dame
 South Bend, U.S.
 emello@nd.edu

2nd Peter Bauer
 Department of Electrical Engineering
 University of Notre Dame
 South Bend, U.S.
 pbauer@nd.edu

Abstract—Realization methods for energy optimal urban driving are the prime focus of this paper. Insights into the real-time generation of such trajectories as well as “in traffic” methods for their execution are provided. This includes the usage of piecewise linear approximations of typical urban speed profiles, urban platooning, filtering of trajectories, and modifying initial accelerations on the trajectory implementation side. On the computation side, precomputed trajectories, and closed-form approximated solutions are investigated.

Keywords—Electric vehicles, energy efficiency, optimized speed profiles, urban platoons

I. INTRODUCTION

The reduction of greenhouse gases, in particular CO₂ emissions, in the future will determine the fate of our planet. The transportation sector is responsible for approximately 30% of all manmade CO₂ emissions and thus is one of the areas where reduction of emissions has a large impact [1]. The transition from fossil fuel-based transportation methods to sustainable transportation will occur on many different fronts, and electrified drivetrains are playing a major part in this transition. Of course, electrified transportation only contributes to a solution to the emission problem if the origin of the power used comes from renewable sources of energy. The work introduced here is based on the assumption of an electrified drivetrain and at least level 2 autonomous driving capability with situational awareness [2].

It has recently been shown [2] that electrified drivetrains in urban environments offer great potential for efficiency improvement by simply optimizing the speed trajectory between stops. The results in [2] point to energy savings of between 30% and 60% depending on vehicle data, drive segment length, speed, etc. However, these results were obtained by simulations that made three key assumptions:

- 100% situational awareness, i.e. exact knowledge of future stops, average speed, etc.
- Other traffic participants do not interfere with the execution of the optimal drive cycle
- Real-time computability can be achieved.

The focus of this paper is on the last two items, i.e. minimizing the effect of other traffic participants (that do not

optimize transportation energy) on achievable efficiency gains, and the timely generation of the optimal speed trajectory. Resolving these issues will be key for maximizing the impact of the concepts proposed in [2], especially during the transition to global energy optimal driving, i.e. for mixed traffic.

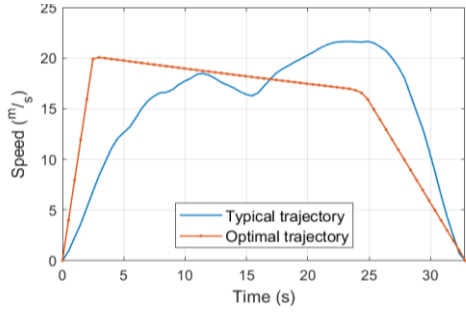
The paper is structured as follows: In section 2 we highlight some of the previous results on energy optimal stop-to-stop speed trajectories that apply to the case of perfect situational awareness. Section 3 provides the problem formulation for this paper concentrating on two major questions. Section 4 provides solutions to the first problem, i.e. optimal trajectories in mixed traffic. The problem of real-time trajectory generation is tackled in section 5, while section 6 provides conclusions and outlook.

II. PREVIOUS RESULTS

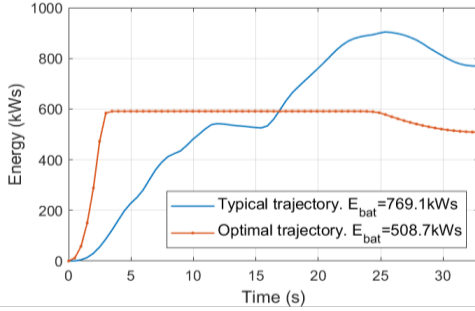
Energy optimal stop-to-stop speed trajectories have been investigated in quite some detail in [2]-[4]. In essence, the problem is to minimize transportation energy at the source, i.e. the battery, when moving from stop to stop with prescribed constraints such as average speed, maximum allowable acceleration, etc. Analytically the problem can be formulated as follows [2]:

$$\begin{aligned}
 & \min_{v_n} \int_0^{t_f} P_{bat}(\tau) d\tau \\
 & \text{s. t. } \int_0^{t_f} v(\tau) d\tau = d \\
 & \quad \frac{d}{t_f} = v_{avg} \\
 & \quad \dot{v}_{min} < \dot{v}(t) < \dot{v}_{max} \\
 & \quad \ddot{v}_{min} < \ddot{v}(t) < \ddot{v}_{max} \\
 & \quad v(0) = 0 \\
 & \quad v(t_f) = 0
 \end{aligned} \tag{1}$$

An example of an optimal speed trajectory is shown in Fig. 1 for a Tesla Model S. Corresponding energy savings relative to a typical FTP 75 derived trajectory is shown to be around 33% in this case. The constraints were given by the average speed (15m/s) and maximum acceleration (8m/s²). It has been shown in [3] that energy savings that can be attained by using this approach are dependent on infrastructural (speed



(a)



(b)

Fig. 1. Energy optimal trajectories (a) speed (b) cumulative energy

limit, average speed, distance) and vehicle (mass, cross-sectional area, coefficient of drag, etc.) data. The powertrain efficiency characteristics also play a significant role in the achievable efficiency gains. In all the previous work, the reference case was a typical stop-to-stop speed profile that was “distilled” from the FTP 75 drive cycle.

III. IMPLEMENTATION PROBLEMS

Obtaining the efficiency gains shown in Fig. 1 requires an exact execution of the optimal speed profile, i.e. a self-driving system is required. In typical urban traffic, executing the optimal speed trajectory is often not possible due to traffic constraints and unforeseen events. In congested urban traffic, speed trajectories are somewhat dictated by other vehicles and optimal trajectories as shown in Fig. 1 are almost impossible to realize. Some mitigation for this problem was suggested in [2], but more realistic concepts are needed. In the section that follows, a few approaches that appear promising are introduced and analyzed.

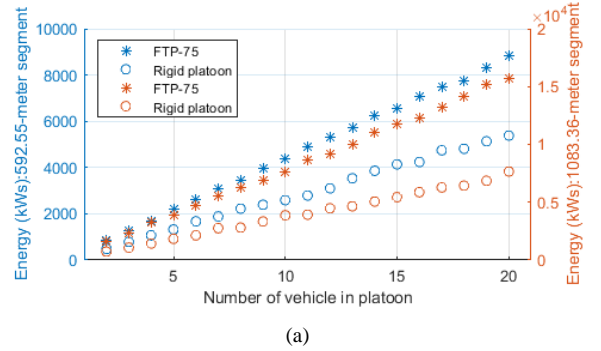
Another aspect of the implementation task is real-time computability. Usually, situational awareness information changes quickly in urban environments and one has only seconds to gather new information and then compute the optimal speed trajectory. Therefore, one must look for approaches that reliably solve the optimization task in a short amount of time. In section V, three different approaches are highlighted and an initial analysis is provided.

IV. REALIZATION APPROACHES FOR EFFICIENCY OPTIMIZED DRIVING

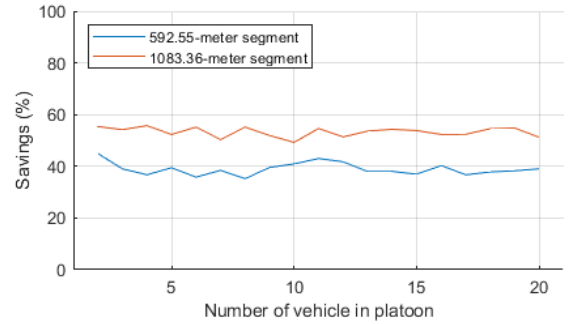
A. Urban platoons

Rather than dealing with mixed traffic problems where autonomous and networked electric vehicles operate among conventional vehicles, generating platoons of similar vehicles that operate optimally and in unison has many advantages

such as decongestion of traffic and the ability to actually execute the optimal trajectory with high probability. In principle there are two types of platoons: a rigid platoon, where following distances are tightly controlled and all vehicles move in unison similar to a train of vehicles, and floating platoons where each vehicle optimizes its own trajectory, thus requiring larger and varying distances between vehicles. Optimized platoons can be generated and realized in several different ways; we will provide several realization options and the associated energy savings compared to conventional non-optimized traffic. Initial simulation results show that while especially in rigid heterogeneous platoons one has some efficiency loss, efficiency is still significantly higher than for conventional driving. The most efficient solution is shown to be the case of rigid homogeneous platoons operating in dedicated lanes. Two examples of this scenario are shown in Fig. 2 (a) that demonstrates the dependency of energy usage on the number of platoon vehicles for a given stop-to-stop segment. The energy savings associated with these platoon realizations are shown in Fig. 2 (b). For the shorter segment, energy savings averaged 39% while for the longer segment, the average savings were equal to 53%.



(a)



(b)

Fig. 2. Typical achievable efficiency gains for a rigid homogeneous platoon using an optimized trajectory.

For the efficient realization of urban platoons, one needs to define criteria for accepting vehicles in the formation. While several admission rules can be defined, we will introduce three options.

1) Minimizing total transportation energy

The first acceptance rule to be discussed is based on the total energy consumption of the platoon. Let $\mathbb{P} = \{V_i \mid i = 1, \dots, N\}$ be the set of vehicles in a platoon of N vehicles. The energy of the platoon between two stops is defined as $E_{s_j}^{s_{j+1}}(\mathbb{P})$ where s_j is the stop of index j in the urban scenario. V_{N+1} is the vehicle to be added to the platoon.

The left-hand side (LHS) of (2) describes the energy consumption of the previous platoon configuration of N

vehicles plus the individual energy of the potential new platoon member. The energy of the new platoon of $N + 1$ vehicles configuration is described in the right-hand side (RHS) of (2).

Therefore, the admittance rule can be stated as:

$$\text{If: } \sum_{j=0}^{N-1} E_{s_j}^{s_{j+1}}(\mathbb{P}) + \sum_{j=0}^{N-1} E_{s_j}^{s_{j+1}}(\{V_{N+1}\}) > \sum_{j=0}^{N-1} E_{s_j}^{s_{j+1}}(\mathbb{P} \cup \{V_{N+1}\}) \quad (2)$$

$$\text{Then: } \mathbb{P}(t + 1) = \mathbb{P}(t) \cup \{V_{N+1}\} \quad (3)$$

$$\text{Else: } \mathbb{P}(t + 1) = \mathbb{P}(t) \quad (4)$$

If in equation (2), the expression in the LHS is greater than the one in the RHS, the vehicle should be accepted to the formation, i.e., equation (3) is true; otherwise, the candidate vehicle should be rejected and (4) is true.

2) Specific parameter intervals

In contrast to the previous strategy, the parameter list acceptance rule is not based on energy consumption but solely on vehicle parameters. \bar{u}_{new} defines the parameter set of a vehicle trying to join the platoon (5).

$$\bar{u}_i = \begin{bmatrix} C_d A \\ m \\ f_r \\ a_{max} \\ a_{min} \end{bmatrix} \quad (5)$$

If $\bar{u}_{min} \leq \bar{u}_{new} \leq \bar{u}_{max}$, the candidate vehicle should be accepted in the platoon as shown in (3); otherwise, the vehicle is rejected, i.e., (4). This is a simple rule to check and enforce; therefore, the platoon composition is predictable and its worst case is easily computable.

3) Individual vehicles voting

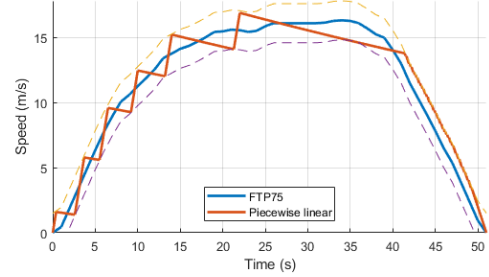
The last proposed acceptance rule is based on individual platoon members evaluating their energy consumption. If the energy expenditure of an individual platoon member were to increase with the addition to the platoon of the to be admitted vehicle, it would vote to not accept the candidate. In contrast, if the individual platoon member were to perceive a reduction in energy consumption, it would vote to accept the candidate vehicle. Different acceptance thresholds are then set based on the current size and heterogeneity of the current platoon, e.g., a majority rule when the platoon is greater than two distinct vehicles. If the set threshold is met, the new vehicle is added to the platoon, i.e., (3) holds. If the threshold is not achieved, the vehicle is rejected and (4) holds.

All three of these approaches will result in different asymptotic compositions. However, it is not clear how this asymptotic behavior is affected by the selection rules.

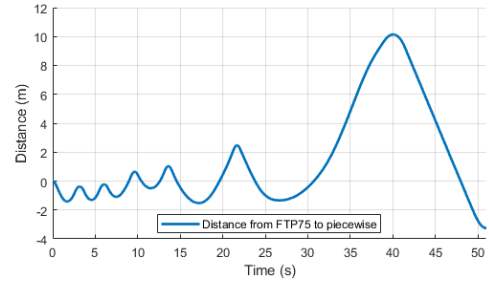
B. Piecewise linear trajectory approximations

For individual vehicles optimization of urban driving speed trajectories, it is necessary to adapt to traffic conditions, especially in dense or congested traffic. A quasi-piecewise linear approximation of a typical FTP 75 stop-to-stop cycle appears to be an interesting approach that can adapt to typical traffic speeds while saving energy.

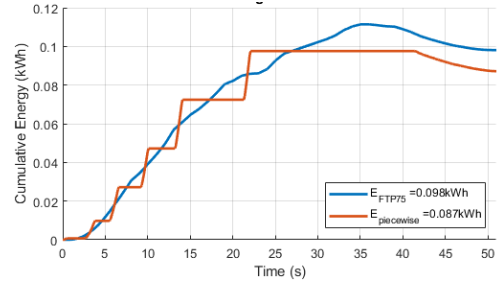
A possible implementation of this approach is shown in Fig. 3 (a) for a vehicle based on a Nissan Leaf. Fig. 3 (b) shows the distance between vehicles and Fig. 3 (c) the cumulative energy consumption to execute each one of the trajectories. For this segment of the FTP 75, the piecewise linear approximation utilizes 11.12% less energy. As demonstrated in [3], optimal speed trajectories achieve greater transportation energy savings for vehicles with higher acceleration capabilities. For that reason, the FTP 75 cycle was approximated by segments of high acceleration (close to the vehicle's limitations) followed by segments of coasting.



(a)



(b)



(c)

Fig. 3. (a) Piecewise linear trajectory approximation of a segment of the FTP75 drive cycle, (b) the distance between lead and following vehicle, and (c) the cumulative energy of each vehicle.

Starting from the force at the vehicle's wheels (6), the coasting deceleration can be calculated by the expression shown in (7).

$$m\dot{v} + mgf_r + \frac{1}{2}CdA\rho v^2 = 0 \quad (6)$$

$$\dot{v} = -gf_r - \frac{1}{2} \frac{CdA}{m} \rho v^2 \quad (7)$$

While the speed from the lead vehicle—which executes the FTP75 drive cycle—is given by $v_1(t)$, the speed from the vehicle executing the quasi-piecewise linear trajectory is given by $v_2(t)$. The difference between those speeds at any

given time is given by $\Delta v(t)$, shown in (8). The limit in variation between speed is then given by Δv_{max} , (9).

$$\Delta v(t) = v_1(t) - v_2(t) \quad (8)$$

$$|\Delta v(t)| < \Delta v_{max} \quad (9)$$

Finally, the distance between vehicles as a function of time can be calculated as shown in (10).

$$\Delta d(t) = \int_0^t v_1(\tau) d\tau - \int_0^t v_2(\tau) d\tau \quad (10)$$

The approach exemplified above is then applied to every segment of the FTP 75 cycle. A series of simulations were calculated where Δv_{max} was varied. The results are shown in Fig. 4. While the bars in blue represent the average savings between each segment of the drive cycle, the bars in red show the overall savings after executing the entire FTP75 drive cycle.

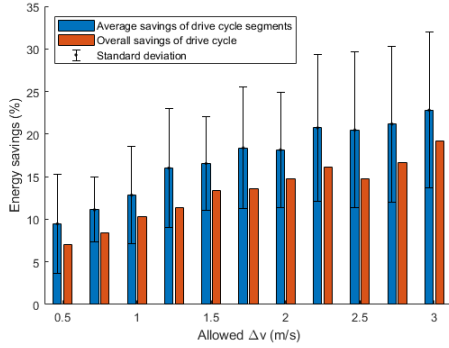


Fig. 4. Energy savings for the piecewise linear trajectory approximation approach as a function of the allowed speed variations.

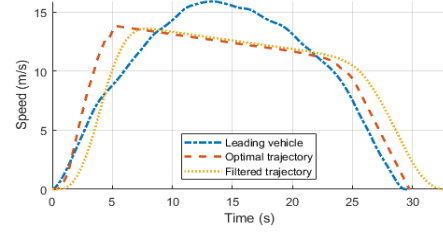
C. Starting delays and trajectory lowpass filtering

As was shown in [2], the combination of a starting delay in combination with a low pass filtered trajectory transforms energy optimal trajectories to more viable trajectories in real traffic. This transformation also takes away the surprise effect a sudden high acceleration of an autonomous driving system may cause where the associated jerk may not be acceptable. A speed trajectory, where filtering was applied, and its respective energy budget are shown in Fig. 5. This figure clearly shows that the delayed and filtered trajectory is not only more smooth but the distance between vehicles can be controlled, i.e. a larger delay and/or a longer low pass filter response creates more distance to the vehicle in front. It should also be noted that the lowpass filtering can be described as the convolution of the optimized trajectory $v(t)$ with an impulse response $h(t)$ (11). While choosing a positive lowpass filter with a DC gain of one (12) would not change the total distance traveled (13), it will slightly reduce the average speed from \bar{v} to $(\bar{v} t_f)/(t_f + \Delta t)$, where Δt is the duration of the filter response. As a consequence, energy is also slightly reduced.

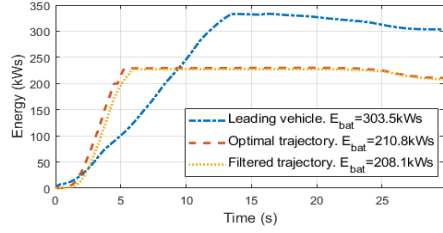
$$v_{new}(t) = v(t) * h(t) \quad (11)$$

$$\int_0^\infty h(\tau) d\tau = 1 \quad (12)$$

$$\int_0^\infty v_{new}(\tau) d\tau = \int_0^\infty v(\tau) d\tau = d \quad (13)$$



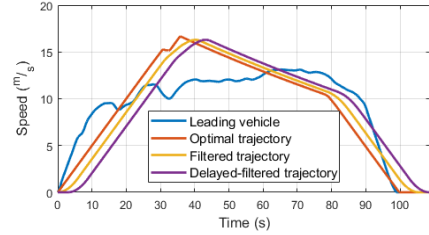
(a)



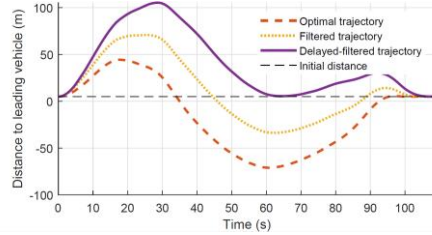
(b)

Fig. 5. LP filtered optimal trajectories and associated energy budget.

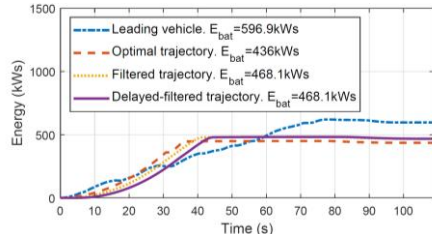
In Fig. 6, a longer optimized segment (1000 meters) demonstrates an optimal trajectory for a vehicle with low acceleration capabilities that was filtered and delayed to maintain a safe distance from the lead vehicle. A six-second filter and a three-second delay were applied. The distance between vehicles $\Delta x(t)$ is shown in Fig. 6 (b) and it can be



(a)



(b)



(c)

Fig. 6. (a) Speed profiles for the lead vehicle, optimized vehicle, optimized vehicle after filtering, and optimized vehicle after filtering and delayed start, as well as (b) the distance between each of the optimized scenarios and the lead vehicle, and (c) the energy budget of each one of the scenarios.

expressed by (14). The initial distance is denoted by Δx_0 and $v_1(t)$ and $v_2(t)$ denote the speed of the lead vehicle and the optimized vehicle, respectively.

$$\Delta x(t) = \Delta x_0 + \int_0^t v_1(\tau) - v_2(\tau - t_0) d\tau \quad (14)$$

D. Lowering initial acceleration

A simple way to adjust to slow congested traffic is to reduce the initial acceleration of the speed trajectory. However, as shown in Fig. 7, reducing the initial acceleration has a significant effect on efficiency. For example, reducing maximum acceleration from 6 m/s² to 4 m/s² reduces energy savings from 44.11% to 40.68%. Further reducing the maximum acceleration to 2 m/s² reduces the savings to 14.72%. Depending on traffic situations, in typical urban traffic, the initial acceleration values are between 1.5m/s² and 2.5m/s². Adapting the optimal speed profile to these values can be, as Fig. 7 shows, not a good solution to the problem since it comes at a high energy penalty. On the other hand Fig. 7 also shows, that vehicles with a high acceleration capability have an advantage and can save more energy than vehicles with lower acceleration. For accelerations above 4 m/s², diminishing returns can be observed.

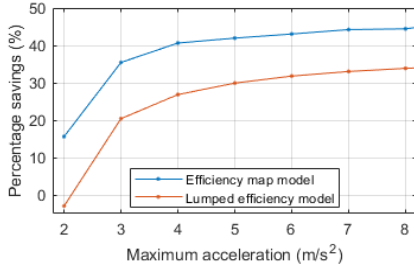


Fig. 7. Energy savings as a function of maximum acceleration for a Tesla Model S in a 500-meter segment at 15 m/s.

V. TRAJECTORY GENERATION

1) Precomputed and stored trajectories

To avoid real-time computation of the optimal trajectory, storing pre-computed trajectories is an attractive option. This section explores the required storage capacity as a function of the sampling rate of segment length, average speed, and initial acceleration. It also provides some guidance concerning the sampling frequency needed, estimated compression gains, and possible interpolation mechanisms.

Typical energy-optimal speed trajectories have between 50 and 300 data points. Each of these data points represents a value of speed. This variation arises from the necessity of storing more data points to represent a long-optimized segment since the trajectory is discretized in time with a fixed time step (Δt). By assuming the upper limit of the necessary data points, e.g., 300 data points, we can calculate an upper bound for the necessary storage capacity. Assuming the data will be stored in 16-bit integers (2 bytes) each trajectory would require 600B of storage.

If one desires to precompute all segments ranging from 100m to 3000m, in 10m intervals, approximately 300 trajectories would be necessary. These trajectories would utilize approximately 175.8 kB. If the average speeds between 3 and 23m/s, in intervals of 1m/s, are desired, approximately 6,000 trajectories are necessary, bringing the necessary

storage capacity to 3.43MB. Finally, if variations of initial and final decelerations are also required, one can subdivide the vehicle capabilities into 16 groups (4 values for the maximum allowed acceleration and 4 values for the maximum allowed deceleration). This brings the total of optimal trajectories to 384,000. All these trajectories can be stored in less than 220MB, posing no burden to any modern computer system.

Even though storing all the trajectories requires little storage, the necessary capacity can be further reduced by utilizing compression algorithms, such as Huffman Coding. This algorithm is estimated to reduce the necessary storage requirement by approximately a factor of ten [5].

Furthermore, an approximation of the optimal speed trajectories can be recreated with only critical points of the original trajectories. The optimal trajectory in Fig. 1 (a) can be subdivided into three distinct segments: acceleration, coasting, and deceleration. By storing the time and speed at the end of each segment, one can easily reconstruct an approximation of the original form. The more complicated optimal trajectories for longer segments shown in [2] can be expressed by additional data points. Each critical point requires 4 bytes to be stored, 2 bytes for the time and 2 for the speed. Assuming an average trajectory requires 10 data points to be expressed, the 384,000 trajectories described before can be stored in around 15MB.

Since the optimal speed trajectories can be closely approximated by linear segments, a linear approximation may provide sufficient accuracy to approximate the original trajectories. More sophisticated interpolation methods may be also implemented. In addition, a polynomial interpolation may be used to approximate the original form whilst also minimizing onsets on acceleration and jerk.

2) Closed-form approximations

Another attractive method to bypass real-time optimization is the usage of linear approximations of the optimal trajectories. For the case where the optimal trajectory consists of only three segments, shown in Fig. 8, the closed-form expressions below will be shown to provide a good approximation for the optimal speed profile.

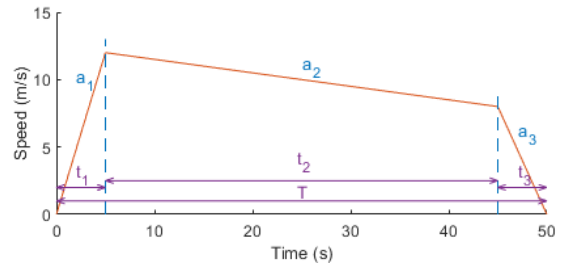


Fig. 8. Sample trajectory for closed-form approximation of a 3-segment optimal speed profile.

For this analysis, the parameter \bar{v} represents the average speed of the optimal trajectory, d the segment length, $a_1 = a_{max}$ the initial acceleration, a_2 the approximated coasting deceleration, and $a_3 = a_{min}$ the braking deceleration. Based on the integral of Fig. 8, the total traveled distance is given by (15).

$$d = \underbrace{\frac{a_1 t_1^2}{2}}_{\text{distance segment 1}} + \underbrace{\frac{2a_1 t_1 + a_2 t_2}{2} t_2}_{\text{distance segment 2}} + \underbrace{\frac{a_1 t_1 + a_2 t_2}{2} t_3}_{\text{distance segment 3}} \quad (15)$$

The total time of the trajectory is defined by (16).

$$t_1 + t_2 + t_3 = T = \frac{d}{\bar{v}} \quad (16)$$

Since the speed trajectory starts and stops at zero speed, (17) must also hold.

$$a_1 t_1 + a_2 t_2 + a_3 t_3 = 0 \quad (17)$$

With some algebraic manipulation, the expressions (18) to (20) for the times t_1 , t_2 , and t_3 can be obtained. Also, based on the average force acting at the wheels of the vehicle, a_2 can be defined as shown in (21).

$$t_1 = \frac{t_2(a_3 - a_2) - a_3 T}{a_1 - a_3} \quad (18)$$

$$t_2 = \sqrt{\frac{2d(a_1 - a_3) + a_1 a_3 T^2}{(a_1 - a_2)(a_3 - a_2)}} \quad (19)$$

$$t_3 = T - t_1 - t_2 \quad (20)$$

$$a_2 = -g f_r - \frac{1}{2} \frac{C_d A}{m} \rho \bar{v}^2 \quad (21)$$

Finally, the total energy consumption of the trajectory can be estimated by (22).

$$E_{bat} = \frac{m a_1 t_1^2}{2\eta} (a_1 + g f_r) + \frac{C_d A \rho a_1^3 t_1^4}{8\eta} \quad (22)$$

In the equations above, the indices show the segment number that the acceleration or time is affiliated with, e.g., a_1 and t_1 are acceleration and duration of segment 1. The accelerations a_1 and a_3 are given by the maximum acceleration and deceleration of the vehicle, η is the power train lumped forward efficiency, the variables \bar{v} , d , and T represent the average speed, segment length, and the total travel time, which are known for a given trajectory. (Regenerative braking efficiency is assumed to be zero.) The variables g , f_r , C_d , A , ρ , and m represent the following vehicle and environmental parameters: gravitational acceleration, coefficient of rolling resistance, air-drag coefficient, vehicle's frontal area, air density, and vehicle's mass, respectively. Finally, the energy utilized by the vehicle is denoted by E_{bat} .

The closed approximation approach above was then applied to segments varying in range from 300 to 800 meters. The results shown in Fig. 9 demonstrate that (22) can produce very good approximations of the energy consumption of an optimal trajectory, especially for short segments. Also, one can conclude that the approximated optimal speed trajectories have very similar energy consumption to the ones obtained from the optimization scheme described in section II. It is important to note that the calculated energy consumption of the closed-form approximations are slightly lower than the energy consumption of the optimized trajectories because they do not obey all the constraints imposed by the optimization scheme.

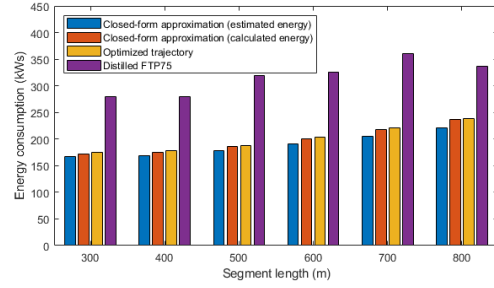


Fig. 9. Energy savings obtained with the closed form approximation of optimal speed profiles.

If a high degree of accuracy is required, neither precomputed optimal speed trajectories nor close form approximations can produce satisfactory results. In this case, the only possible method for generating the optimal speed trajectories in a timely fashion would be cloud computing utilizing V2I communication. Such an approach should be feasible in urban scenarios [6].

VI. CONCLUSION AND OUTLOOK

This paper introduces a variety of concepts that facilitate the implementation of energy optimal urban speed profiles under dense traffic conditions. The analysis focuses on two major issues: (a) trajectory implementation, modification, and adaptation to traffic conditions, and (b) computability, and real-time trajectory generation. In the former, urban energy optimal platoons, piecewise linear trajectory approximations, filtered optimal speed trajectories, and reduced initial accelerations, were methods investigated. In the latter, considered solutions were closed-form approximations, and precomputed and parameterized trajectory sets. While all investigated approaches are effective, it can be concluded that urban platoons and precomputed/closed-form trajectories are among the most promising solutions.

In general, the aspects detailed in this paper have the goal of reducing the complexity involved in generating energy-optimal speed trajectories and making them more easily implementable while maintaining high energy savings.

REFERENCES

- [1] U.S. Environmental Protection Agency (EPA), "Fast Facts: U.S. Transportation Sector Greenhouse Gas Emissions", June 2019. [Online]. Available: <https://nepis.epa.gov/Exe/ZyPDF.cgi?Dockkey=P100WUHR.pdf>. [Accessed: Feb. 6, 2020].
- [2] E. F. Mello and P. H. Bauer, "Energy-Optimal Speed Trajectories Between Stops," in IEEE Transactions on Intelligent Transportation Systems. doi: 10.1109/TITS.2019.2939776
- [3] P. H. Bauer and E. F. Mello. "Sustainability in Electric Transportation: Minimizing Transportation Energy". In: Volume 1: Proceedings of Applied Energy Symposium: MIT A+B, AEAB2019, Boston, MA, May 22-24. (In Progress). 2019.
- [4] E. F. Mello and P. H. Bauer, "Energy-optimal Speed Trajectories between Stops and Their Parameter Dependence", in VEHITS, Heraklion, Crete – Greece. DOI:10.5220/0007747605130520
- [5] K. Sayood, *Introduction to data compression*. San Francisco, CA, USA: Morgan Kaufmann Publishers, 2006.
- [6] Y. Wang, K. Venugopal, A. F. Molisch and R. W. Heath, "MmWave Vehicle-to-Infrastructure Communication: Analysis of Urban Microcellular Networks," in IEEE Transactions on Vehicular Technology, vol. 67, no. 8, pp. 7086-7100, Aug. 2018, doi: 10.1109/TVT.2018.2827259.